Bioactive Materials 26 (2023) 425–436

Contents lists available at ScienceDirect

Bioactive Materials

journal homepage: www.keaipublishing.com/en/journals/bioactive-materials

# miR-204 ameliorates osteoarthritis pain by inhibiting SP1-LRP1 signaling and blocking neuro-cartilage interaction

Ke Lu [a,b,1], Qingyun Wang [a,b,1], Liuzhi Hao [c], Guizheng Wei [a,b], Tingyu Wang [d], William W. Lu [b,e], Guozhi Xiao [f], Liping Tong [a], Xiaoli Zhao [c,**], Di Chen [a,b,*]

[a] Research Center for Computer-aided Drug Discovery, Shenzhen Institute of Advanced Technology, Chinese Academy of Sciences, Shenzhen, 518055, China
[b] Faculty of Pharmaceutical Sciences, Shenzhen Institute of Advanced Technology, Shenzhen, 518055, China
[c] Research Center for Human Tissues and Organs Degeneration, Shenzhen Institute of Advanced Technology, Chinese Academy of Sciences, Shenzhen, 518055, China
[d] Department of Pharmacy, Shanghai Ninth People's Hospital, Shanghai Jiao-Tong University School of Medicine, Shanghai, 200011, China
[e] Department of Orthopaedics and Traumatology, The University of Hong Kong, Hong Kong 999077, China
[f] School of Medicine, Southern University of Science and Technology, Shenzhen, 518055, China

ARTICLE INFO

*Keywords:*
miR-204
LRP1
Neuro-cartilage interaction
Osteoarthritis
Pain

ABSTRACT

Osteoarthritis (OA) is a painful degenerative joint disease and is the leading cause of chronic disability among elderly individuals. To improve the quality of life for patients with OA, the primary goal for OA treatment is to relieve the pain. During OA progression, nerve ingrowth was observed in synovial tissue and articular cartilage. These abnormal neonatal nerves act as nociceptors to detect OA pain signals. The molecular mechanisms for transmitting OA pain in the joint tissues to the central nerve system (CNS) is currently unknown. MicroRNA miR-204 has been demonstrated to maintain the homeostasis of joint tissues and have chondro-protective effect on OA pathogenesis. However, the role of miR-204 in OA pain has not been determined. In this study, we investigated interactions between chondrocytes and neural cells and evaluated the effect and mechanism of miR-204 delivered by exosome in the treatment of OA pain in an experimental OA mouse model. Our findings demonstrated that miR-204 could protect OA pain by inhibition of SP1- LDL Receptor Related Protein 1 (LRP1) signaling and blocking neuro-cartilage interaction in the joint. Our studies defined novel molecular targets for the treatment of OA pain.

## 1. Introduction

Osteoarthritis (OA) is a painful degenerative joint disease and is the leading cause of chronic disability among elderly individuals. A key aspect of improving health-related quality of life among patients with OA is to ameliorate OA-related pain before surgical interventions. Previous studies have established multiple signaling pathways and signaling molecules, such as Indian Hedgehog (Ihh), transforming growth factor β (TGF-β), β-catenin and Runx2, are involved in the pathological process of OA, mainly by directly or indirectly affecting anabolic or catabolic process in cartilage [1–4]. However, the molecular mechanisms of OA nociception remain poorly understood.

The dorsal root ganglia (DRG) is responsible for transmitting peripheral pain signals to the central nervous system (CNS) after chemical, mechanical or thermal stimulation [5]. During OA progression, vascular invasion and nerve ingrowth could be detected in synovial tissue and articular cartilage [6]. These abnormal neonatal nerves act as nociceptors to sense OA pain signals and could directly excite DRG nociceptive neurons [6]. Several recent studies have demonstrated that the immune cells and other non-neural cells produce pro-inflammatory cytokines, such as interleukin-1 (IL-1) and tumor necrosis factor (TNF), causing inflammatory pain in OA [7]. To date, few studies have investigated the crosstalk between chondrocytes and neural cells during OA pain induction.

Our previous study has identified two homologous microRNAs, miR-204 and miR-211, acting as negative regulators of Runx2 gene and play a

Peer review under responsibility of KeAi Communications Co., Ltd.
* Corresponding author. Faculty of Pharmaceutical Sciences, Shenzhen Institute of Advanced Technology, Shenzhen, 518055, China.
** Corresponding author.
*E-mail addresses:* zhao.xl@siat.ac.cn (X. Zhao), di.chen@siat.ac.cn (D. Chen).
[1] These authors contributed equally to this work.

https://doi.org/10.1016/j.bioactmat.2023.03.010
Received 2 November 2022; Received in revised form 14 March 2023; Accepted 15 March 2023
Available online 20 March 2023

critical role in maintaining joint tissue homeostasis [8]. It is well known that exosomes carry bio-macromolecules and play important roles in physiological intercellular crosstalk as well as disease pathogenesis [9]. Previous studies have suggested that exosomes possess good biocompatibility and biodegradability, and protect miRNAs from degradation [10].

In this study, we investigated the interaction mechanisms between chondrocytes and neural cells and evaluated the effect of miR-204 delivered by exosome mimetics in the treatment of OA and associated pain in an experimental OA mouse model. Our findings demonstrated that miR-204 could protect OA pain by inhibition of SP1-LRP1 signaling and neuro-cartilage interaction in the joint.

## 2. Materials and methods

### 2.1. Cells and cell culture

Human chondrocyte cell line C28/I2 (SSRCC, China), human embryonic kidney cell line 293 cells (HEK293) (ATCC, USA) and human Schwann cell line ipNF95.11 b C (ATCC, USA) were cultured according to vendor's instruction. Human mesenchymal stem cells (hMSCs) were purchased from Cyagen (HUXMA-01001, USA) and cultured in oriCell™ human Mesenchymal Stem Cell growth media (HUXMA-90011, Cyagen Biosciences) containing 10% fetal bovine serum (FBS; Gibco, USA). The 2nd passage cells were used for subsequent experiments. C28/I2, HEK293 and ipNF95.11 b C cells were cultured in Dulbecco's modified Eagle's medium (DMEM) supplemented with 10% FBS and penicillin (100 U/ml). All the cells were incubated at 37 °C and 5% $CO_2$ in a humidified incubator.

For the co-culture of C28/I2 and ipNF95.11 b C cells, C28/I2 cells in the upper layer were transfected with *SP1* siRNA or *SP1* plasmid for 6 h, then transmitted to wells with ipNF95.11 b C cells and co-cultured for 24 h.

MicroRNA, miR-204 mimic (Sangon Biotech, Shanghai, China), or *SP1* siRNA were transfected into C28/I2 cells using Lipofectamine RNAi MAX transfection reagent (Life Technologies, Grand Island, NY, USA). *RSV-SP1* (Addgene, USA) was infected into chondrocytes and HEK293 cells at a concentration of 50 nM. Empty vectors or scramble siRNA were used as negative controls as indicated.

### 2.2. Exosomes isolation, exosome-mimetic preparation and miR204 loading

Human mesenchymal stromal cells (hMSCs) were used to collect exosome and generate exosome-mimetics (EM). Exosomes were collected from exosome-free culture medium. Briefly, medium supernatant was centrifuged at 10,000×*g* to remove cell debris and then centrifuged at 100,000×*g* to collect exosome. The obtained exosomes were suspended in PBS and stored at −80 °C for further use. Cells were collected and suspended at a concentration of $1 \times 10^6$ cells $mL^{-1}$. Sequential extrusion was then used to fabricate cells to nano-sized vesicles through 5, 1 and 0.2 μm polycarbonate membranes (Nuclepore, Whatman) by a mini-extruder. Cell debris were removed by centrifugation at 10,000×*g* for 20 min. EM were concentrated by 100 kDa ultracentrifugal filter (Millipore, Merck). Electroporation method was applied for miR-204 loading by Gene Pulse Xcell system (Bio-rad). Briefly, 10 μgEM and 25 pmol miR-204 were mixed in a 4 mm cuvette with electroporation buffer (Millipore, Merck). The electroporation voltage was set as 100 V for 10 ms. Unloaded miR-204 was removed by 100 kDa ultracentrifugation tubes and stored at −80 °C for further use. The morphology of exosomes and EM were observed by transmission electron microscopy (TEM). The size and zeta potential of exosomes and EM were analyzed by Nano ZS. Exosomal marker of exosomes and EM, including TSG101, CD81 and CD9, were analyzed by western blot assay.

### 2.3. Western blot

Western blot was performed as described previously [11]. Briefly, protein samples were extracted from cells or exosomes. After separation, samples were electro-transferred onto fit PVDF membranes (Bio-Rad, Hercules, California, USA). The membranes were blocked in 3% Non-fat milk and incubated with primary antibodies at 4 °C overnight. After incubated with secondary antibodies for 1 h at room temperature and washed in PBST for 30 min the membranes were exposed to SuperSignal West Pico Chemiluminescent Substrate (Thermo Scientific, Waltham, Massachusetts, USA) and visualized by radiography. The antibodies used in this study were listed in online Supplemental Table S1.

### 2.4. Pain-related behavior tests

To examine the long-term movements of mice, the Laboratory Animal Behaviour Observation, Registration, and Analysis System (LABORAS™, Metris, Hoofddorp, The Netherlands) was used, according to protocols as previously described [12,13]. Briefly, mice were placed in 4 individual cages with unlimited access to food and water. The sensor platform electronically measures the mechanical vibrations caused by the movement of the animal. Assays started from 20:00 p.m. first day until 8:00 a.m. of next morning for 12 h. The parameters analyzed include motion track, distance moved, speed, locomotion, immobility, climbing and rearing. Recorded data were taken and calculated using LABORAS 2.6 software (Metris, Netherlands).

To determine changes in mechanical allodynia, von Frey tests were performed using a calibrated set of von Frey filaments (North Coast Medical Inc., CA, USA) as previously described [12,13]. Before von Frey hind paw test, the mice were placed in testing chambers on elevated wire grid for an hour to acclimatize. A reaction that the mice exhibit any withdraw behavior will be considered as a positive response. The set of von Frey filaments started from 0.6 g were used to poke from below the hind paw to calculate the 50% force withdrawal threshold using an iterative approach. The tests were performed in a blind manner in that the investigators were not aware of the identification of animals as well as the study groups.

### 2.5. Micro-CT analysis

After the mice scarified, the right knee joints were fixed in 4% formaldehyde overnight and washed by PBS before scanning. We used a NEMO Micro-CT scanner (Pingsheng Healthcare Shanghai Inc., Shanghai, China) with 90 kV source and 70 μA current for formalin-fixed mouse legs with a resolution of 10 μm. The scanned images from each group were evaluated at the same thresholds to allow 3-dimensional structural rendering of each sample. The region below the cartilage to growth plate of subchondral bone in proximal tibia was selected for 3-dimensional histomorphometric analysis to determine cortical or subchondral bone mineral density (BMD), trabecular bone volume per tissue volume (%, BV/TV), trabecular number (Tb.N.), trabecular spacing (Tb.Sp.), and trabecular thickness (Tb.Th.).

### 2.6. Histological analysis

For histology and IHC, right knee joints were fixed in 10% formalin, decalcified in formic acid, and embedded in paraffin. Serial coronal sections of knee joints were cut every 5 μm from the medial compartments. The sections were stained with safranine o/fast green for histological analysis. OARSI scoring was performed to evaluate articular cartilage destruction essentially as previously described [12–14].

For IHC or IF staining, after rehydrated and antigen retrieval, the sections were then sequentially treated with Endogenous Peroxidase Blocking Buffer (Beyotime, China), 0.5% Triton X-100, Avidin/Biotin Blocking Kit and incubate with primary antibodies over night at 4 °C. For IHC staining, the sections were incubated with secondary

biotinylated antibodies for 1 h, and followed by treatment with the VECTASTAIN Elite ABC Kit and revealed IHC signals by ImmPACT DAB Peroxidase Substrate. For IF staining, the sections were incubated with peroxidase-conjugated anti-fluorescein antibodies and mounted by VECTASHIELD Mounting Medium with DAPI (Vector Laboratories, Burlingame, CA, USA). Images of histology, IHC and IF were captured using CellSens Imaging Software on an Olympus IX71 microscope. The average intensity was analyzed using ImageJ program. The antibodies used in IHC and IF were also listed in Table S1.

LC-MS/MS analysis was performed on an Ultimate 3000 nano RSLC system connected to a Qexactive Plus mass spectrometer (both Thermo Fisher Scientific, Waltham, MA, USA) by LC-Bio Technology Co., Ltd. (Hangzhou, China). Briefly, cellular proteins were extracted by lysis buffer (8 M Urea, 1% protein inhibitors mixture) and quantified by BCA kit. Samples were then added DTT (30 °C reaction for 60min) to reduce disulfide bonds, and added iodoacetamide (IAM) to enclose the free thiol group avoiding light at room temperature for 45min. For protein digestion, samples were resolubilized in 100 μL denaturation buffer (50 mM triethylammonium bicarbonate (TEAB) in 50/50 trifluoroethanol (TFE)/$H_2O$ (v/v)) by pipetting and ultrasonication. Then the samples were enzymatically digested overnight by trypsin, 37 °C. Finally, the peptides were desalted with C18 SPE column dried with a vacuum concentrator and solubilized in 0.05% trifluoroacetic acid and 2% acetonitrile in water by pipetting, vortexing, and ultrasonication. Samples were filtered through 0.2 μm spin filter, transferred to HPLC vials, and stored at −80 °C until LC–MS/MS analysis.

Mass spectrometry Raw format files are retrieved directly using Maxquant (v.1.5.2.8). The search parameters are set as follows: tandem mass spectra were searched against the UniProt databases of Homo sapiens (2018/02/02; http://www.uniprot.org/proteomes/UP000005640); the digestion mode is set to Trypsin/P; TMT quantification, maximum number of allowable missing shear sites2, FDR less than or equal to 0.01 first-order mother ion mass error tolerance set to 10 ppm; the mass error tolerance of the secondary fragment ions is set to 0.02 Da; fixation modifications are set to cysteine alkylation; the variable modification is set to oxidation of methionine, Deamidation (NQ), acetylation of the N-terminal of the protein.

### 2.7. RNA extraction and quantitative real-time PCR

Total RNA was extracted from cells with NucleoZol according to the manufacturer's protocol (Invitrogen, USA) and reverse transcribed by a RT reagent kit (Takara, Japan). Specifically, the reverse transcription primer of miR-204 was (5′-GTCGTATCCAGTGCAGGGTCCGAGGTATTCGCACTGGATACGACAGGCAW-3′). The cDNA was subjected to SYBR Green-based real-time PCR analysis on an Applied Biosystems by Thermo Fisher Scientific. All quantification was performed in triplicates and normalized to an endogenous β-actin control. *LRP1, SP1, NGF, ADAMTS5, CGRP, MMP13* and *COLX* expression were detected. The primer sequences were listed in Table S2.

### 2.8. Flow Cytometry

MSCs and C28/I2 cells were treating with Dil-EMs for 2 h. Then the cell suspensions were collected and tested using a BD LSRFortessa Flow Cytometry. Flow data were then analyzed using FlowJo software.

### 2.9. In vivo imaging analysis

For tracking EMs biodistribution and migration after intra-articular injection, Dil labeled exosome mimetics (EMs) were intra-articularly injected into 10-week-old C57BL/6 mice. 5 min, 24, 48, 72, 96 and 120 h later, the mice were anesthetized for ex vivo fluorescence imaging using an *in vivo* imaging system (IVIS Spectrum, PerkinElmer, CA).

### 2.10. Animal studies

Ten-week-old male and female C57BL/6 mice were purchased from GemPharmatech (Nanjing, China). Mice were divided into four groups (n = 5 in each group), Ctrl group: Sham operation with PBS injection, DMM surgery with PBS injection, DMM surgery with injection of EMs alone, DMM surgery with injection of $EMs^{miR-204}$. The EMs or $EMs^{miR-204}$ were delivered by the exosome. DMM surgery was performed as previously described [15]. Briefly, after anesthetizing the mice, the medial meniscotibial ligament is transected to destabilize the joint. The control group underwent Sham surgery in which a similar incision was made into the joint capsule and then closed. All the mice were kept in a specific pathogen-free facility (SPF) in individual ventilation cages, 5 mice per cage, and the animals were in a 12 h day/night cycle and a controlled housing temperature at 22 °C. Caging, food, and water bottles were changed weekly. All mice were allowed to rest for 2 weeks after surgery, followed by the intra-articular injection of PBS, EMs or $EMs^{miR-204}$, every two weeks (15 μg $EMs^{miR-204}$ per injection per mouse) for 8 weeks (Fig. S1) according to pilot experiment. The injection strategy was based on the information of *in vivo* imaging which indicated that EMs could sustain for at least 5 days (Fig. S2). To avoid disturbing knee joint frequently, we chose bi-weekly injection and found this treatment regimen is effective for OA pain protection. The animal protocol of this study has been approved by Ethics Committee of the Shenzhen Institute of Advanced Technology, Chinese Academy of Sciences and all experimental methods and procedures were carried out in accordance with the approved protocol to comply with all ethical regulations for animal testing and research (SIAT-IACUC-210618-YYS-CD-A1955).

### 2.11. Statistical analysis

Statistical analyses were conducted using Prism GraphPad Prim 8.0 software. All the data were expressed as mean ± S.D., as indicated in the figure legends. Unpaired Student's *t*-test (for two groups), one-way ANOVA (for multiple groups with one variable factor) and two-way ANOVA (for multiple groups with two variable factors) were used followed by the Tukey post-hoc test. Correlations were assessed using Pearson's rank correlation test. All experiments were performed and analyzed using 3 individual samples, unless otherwise mentioned. $P < 0.05$ was considered statistically significant and is denoted in the figures. The experiments were randomized, and the investigators were blinded to allocation during experiments and outcome assessment.

## 3. Results

### 3.1. Efficient delivery of miR-204 to chondrocytes by bone marrow mesenchymal stromal cell-derived exosomes mimetics

To prepare $EMs^{miR-204}$, we performed electroporation to load miR-204 into exosome mimetics (EMs) which were collected by serial extrusion of hMSCs (Fig. 1A). The electron microscopy observation showed the diameter of $EMs^{miR-204}$ was around 100 nm (Fig. 1B and C). To further characterize the exosomal marker proteins, we performed immunoblots and found CD9, CD81and TSG101 were enriched in exosomes and EMs (Fig. 1D). The average size of $EMs^{miR-204}$ was about 8% larger than empty EMs without carrying miR-204 (Fig. 1E). The zeta potential of $EMs^{miR-204}$ and EMs showed no statistically significant difference (Fig. 1F). We performed qPCR and found the *miR-204* levels were significantly increased in $EMs^{miR-204}$ transfected chondrocytes compared with that in EMs alone transfected chondrocytes (Fig. 1G). The loading efficiency of *miR-204* in exosomes was more than 80% (Fig. S3A). The release kinetics exosomal *miR-204* showed that *miR-204* levels were decreased from 12 h after transfection in chondrocytes and decreased to the baseline level 72 h after transfection (Fig. S3B). To determine if $EMs^{miR-204}$ could be efficiently uptake by chondrocytes, we

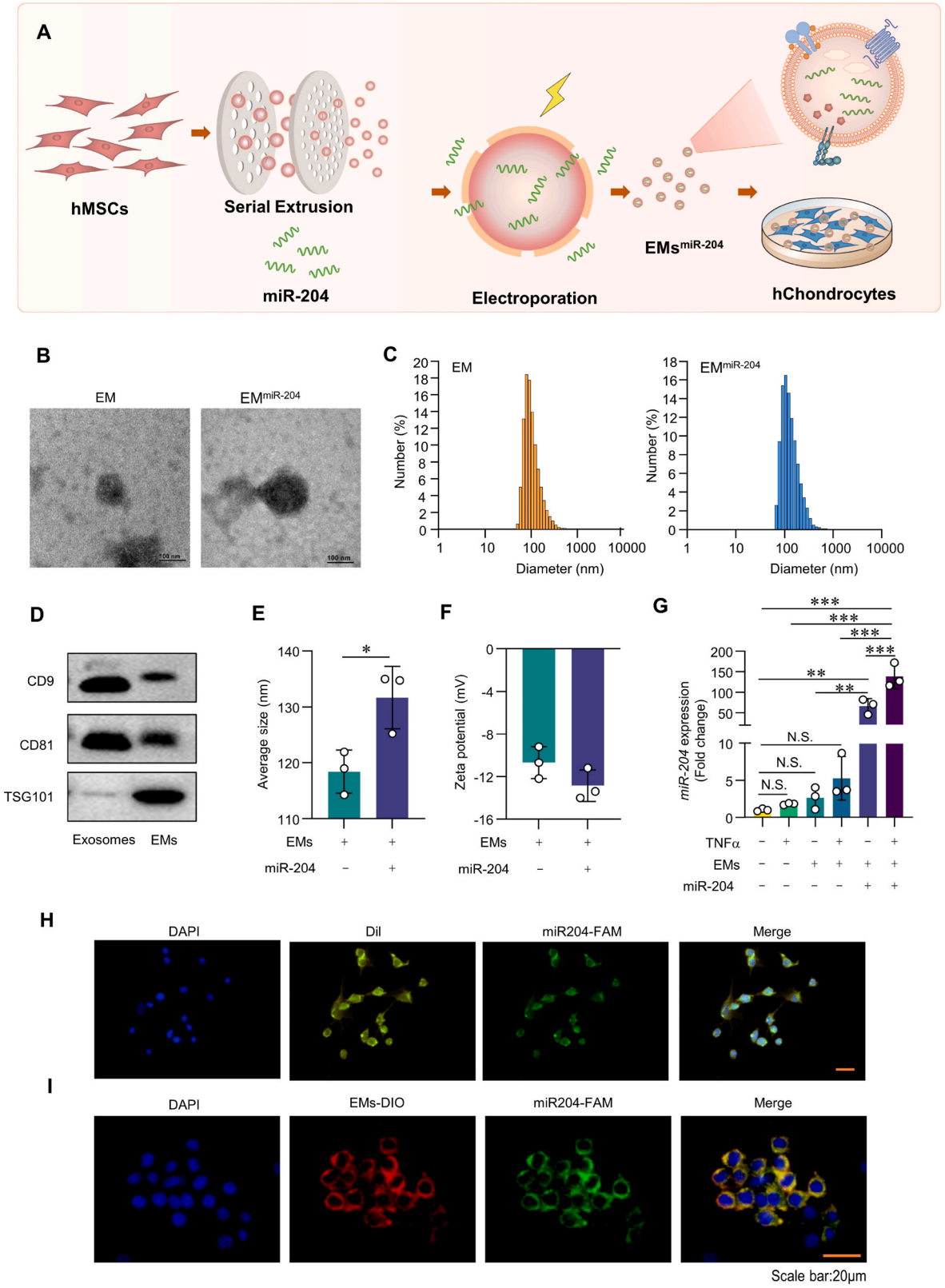


**Fig. 1.** Bone marrow mesenchymal stem cell-derived exosomes mimics efficiently deliver miR-204 to target chondrocytes. (A) A schematic diagram illustrating the extrusion of exosome mimetics and electroporation of *miR-204*. (B and C) The representative images of electron microscopy (B) and diameter analysis (C) of EMs and EMs$^{miR-204}$. (D) Representative immunoblots of CD9, CD81, TSG101 in exosomes and EMs (n = 3). (E and F) Average size (E) and Zeta potential (F) of EMs and EMs$^{miR-204}$ (n = 3). (G) qPCR analysis of *miR-204* expression in C28/I2 cells treated with EMs or EMs$^{miR-204}$ as indicated (n = 3). (H and I) Representative immunofluorescent (IF) images showing EMs$^{miR-204}$ enter into the C28/I2 cells (H) and located around nuclei (I). Purified EMs were labeled with the dye DIO. miR-204s were labeled with FAM. Dil was used to stain cell membranes. DAPI was used to stain nuclei. *: $P < 0.05$, **: $P < 0.01$, ***: $P < 0.001$, N.S.: no significant difference. Data are represented as mean ± SD. Two-tailed Student's unpaired *t*-test analysis (E and F). One-way ANOVA followed by Tukey post-hoc test for multiple comparisons (G).

used DIO (a membrane dye for EM labeling) and FAM (a fluorescent dye for miRNA labeling) to label EMs$^{miR-204}$. Dil was used to stain cell membranes. Immunofluorescent (IF) staining showed EMs$^{miR-204}$ could enter into chondrocytes (Fig. 1H) and located around the nuclei (Fig. 1I). *miR-204* could be delivered by EM to both chondrocytes and MSCs (Figs. S4A and B)

### 3.2. Treatment with EMs$^{miR-204}$ relieves pain in OA mouse model

To determine if EMs$^{miR-204}$ could be used to treat osteoarthritic pain, we performed DMM surgery in 10-week-old C57 mice to create an OA mouse model and administered EMs$^{miR-204}$ by intra-articular injection every two weeks after DMM surgery. Intra-articular injection of EMs alone was used as a control. Dil stained EMs could last for at least 5 days after one-time intra-articular injection using *in vivo* imaging tracking system to detect EMs (Fig. S2). We then performed von Frey test to evaluate changes in mechanical allodynia in the mice treated with EMs$^{miR-204}$ and found lower von Frey scores (reflecting increased pain sensitivity) after DMM surgery and this effect could be partially reversed by the treatment with EMs$^{miR-204}$ compared to those in the control mice treated with EMs alone (Fig. 2A). We then analyzed changes in spontaneous activities using LABAROS and found reduced spontaneous activities after DMM surgery, including changes in locomotion, climbing, rearing, walking distance and speed and the improvement of spontaneous activities in the mice treated with EMs$^{miR-204}$ (Fig. 2B–G, Figs. S5A–E). Some parameters of spontaneous activities, such as walking distance in the cages (Fig. 2F) and average speed of animal walking (Fig. 2G) were significantly increased in EMs alone group, suggesting that EMs alone have partial effect on pain relief. In contrast, EMs$^{miR-204}$ group showed further increases in these parameters. This is not a surprise because EMs have been showed its positive effects on cartilage repair in previous studies [16]. The joint injury caused by OA is detected as pain signals by the ingrowth of somatosensory neurons (nociceptors) innervating tissues (joint depicted) for which the cell bodies are clustered in dorsal root ganglia (DRG) (Fig. 2H). These signals are carried to the dorsal horn of the spinal cord and then transmitted to the brain via central axonal terminals (Fig. 2H). Results of IF staining showed that expression of neuron markers PGP9.5, TUJ1, NGF and CGRP was increased after DMM surgery in the joint tissues and administration of EMs$^{miR-204}$ suppressed expression of neuron makers (Fig. 2I-M). These findings indicate that intra-articular injection of EMs$^{miR-204}$ has beneficial effect to alleviate osteoarthritic pain in murine DMM model through inhibition of nociceptor invasion in the junction area of synovial membrane and cartilage.

### 3.3. LRP1 was identified as a downstream molecule of miR-204, which is involved in pain signaling regulation in chondrocytes

Our previous study demonstrated that deficiency of *miR-204/-211* in mesenchymal progenitor cells recapitulates OA pathogenesis [8]. To further investigate how *miR-204* targets chondrocytes and regulate pain signaling in nociceptive neurons, we conducted LC-MS/MS based proteomic profiling studies. We treated chondrocytes with TNF-α to induce inflammatory response and administered EMs$^{miR-204}$ to inhibit the effects of TNF-α. Chondrocytes treated with TNF-α+EMs alone were used as a control. 665 up-regulated proteins and 803 down-regulated proteins were identified in chondrocytes by the treatment with EMs$^{miR-204}$ (Fig. 3A). The down-regulated proteins were mainly involved in inorganic ion homeostasis, cation homeostasis, glycerophospholipid metabolic process, which also overlapped with transmembrane transport signaling proteins (Fig. 3B). Consistent with these findings, cellular component and molecular functional analysis also showed that transmembrane transporter activity may contribute to the *miR-204*-mediated pain signaling transduction to nociceptor, from chondrocytes treated with EMs$^{miR-204}$ (Fig. 3C, Figs. S6A and B). Down-regulated proteins in KEGG pathway and COG/KOG category analyses also established that signals related to transmembrane transporter activity may contribute to pain alleviation regulated by miR-204 (Figs. S7A and B).

To screen the candidate(s) that could be involved in both *miR-204* regulated molecules and pain signaling proteins, we analyzed the overlapping between 803 down-regulated proteins in chondrocytes treated with EMs$^{miR-204}$ or chondrocytes treated with EMs alone and 94 pain related molecules (Fig. 3D, Table S3). Finally, five genes (*DNMT1, LRP1, MAOA1, SPTLC1, SPTLC2*) were identified and were further investigated. We found that the expression of *DNMT1*, *MAOA1* and *SPTLC2* was not decreased in chondrocytes treated with EMs$^{miR-204}$ compared with that in chondrocytes treated with EMs alone (Figs. S8A–C). Interestingly, the expression of *LRP1*and *SPTLC1,* two known neuron growth related genes, was significantly decreased in chondrocytes treated with EMs$^{miR-204}$ compared with that in chondrocytes treated with EMs alone (Fig. 3E and F). Because *Lrp1* showed more dramatic decrease (more than 50%) after *miR-204* treatment, we decided to further investigate the role of LRP1 in *miR-204* signaling in OA pain. Results of IF staining revealed that LRP1 levels were increased at the junction area of synovial membrane and cartilage in DMM mice. In contrast, LRP1 expression was decreased in DMM mice treated with EMs$^{miR-204}$ compared with DMM mice treated with EMs alone (Fig. 3G and H).

### 3.4. miR-204 down-regulates LRP1 expression through inhibition of transcription factor SP1

To further explore the molecular mechanisms underlying miR-204 down-regulation of pain-related genes expression, we performed bioinformatics analysis of transcription factors that may bind to the *LRP1* and *SPTLC1* promoters with information obtained from database of *miR-204* targeting genes. 9 transcription factors (*CREB1, DRAP1, EGR1, IKZF5, RBFOX2, SP1, ZEB1, ZNF335, ZNF792*) were identified for further analysis (Fig. 4A). We then performed *in vitro* study to determine the expression patterns of these transcription factors. We found the mRNA levels of *CREB1, DRAP1, EGR1, SP1, ZEB1* and *ZNF335* were significantly decreased in chondrocytes treated with EMs$^{miR-204}$ compared with those in chondrocytes treated with EMs alone (Fig. 4B and Figs. S9A–H). We then decided to focus on *SP1* in regulation of LRP1. Results of qPCR and immunoblotting showed that expression of *SP1* mRNA and protein was decreased in chondrocytes treated with EMs$^{miR-204}$ compared with that in chondrocytes treated with EMs alone (Fig. 4C).

We next determined how SP1 regulates LRP1 expression. We infected RSV-*SP1* plasmid into chondrocytes and found high expression of *SP1* mRNA and protein levels compared with those in the cells infected with RSV alone (Fig. 4D–F, Fig. 4G and H). We then performed ChIP assay. SP1 binding DNA fragments were harvested for ChIP assay. We found high level of SP1 binding to the *LRP1* promoter in the cells infected with RSV-*SP1* (Fig. 4I). We also performed luciferase reporter assay and found that luciferase activity was decreased in chondrocytes when mutant *LRP1-Luc* construct (mutation in SP1 binding site in the *LRP1* promoter) was transfected into chondrocytes compared with that when WT *LRP1-Luc* construct was transfected into chondrocytes (Fig. 4J). We also used *SP1* siRNA (*siSP1*) to down-regulate *SP1* expression under TNF-α stimulation in chondrocytes (Fig. 4K-M). Consistent with the inhibitory effect of EMs$^{miR-204}$, we found that *LRP1* mRNA and protein levels were also decreased in chondrocytes with *SP1* siRNA transfection in the presence of TNF-α (Fig. 4N-P).

### 3.5. The EMs$^{miR-204}$ inhibits SP1-LRP1 signaling in chondrocytes and down-regulates nociceptive neuron activation

To further determine the role of miR-204 regulated SP1-LRP1 signaling in regulation of nociceptive neuron, we conducted chondrocytes and Schwann cells co-culture experiments. The upper layer of cells (chondrocyte cell line, C28/I2) were transfected with *SP1* siRNA

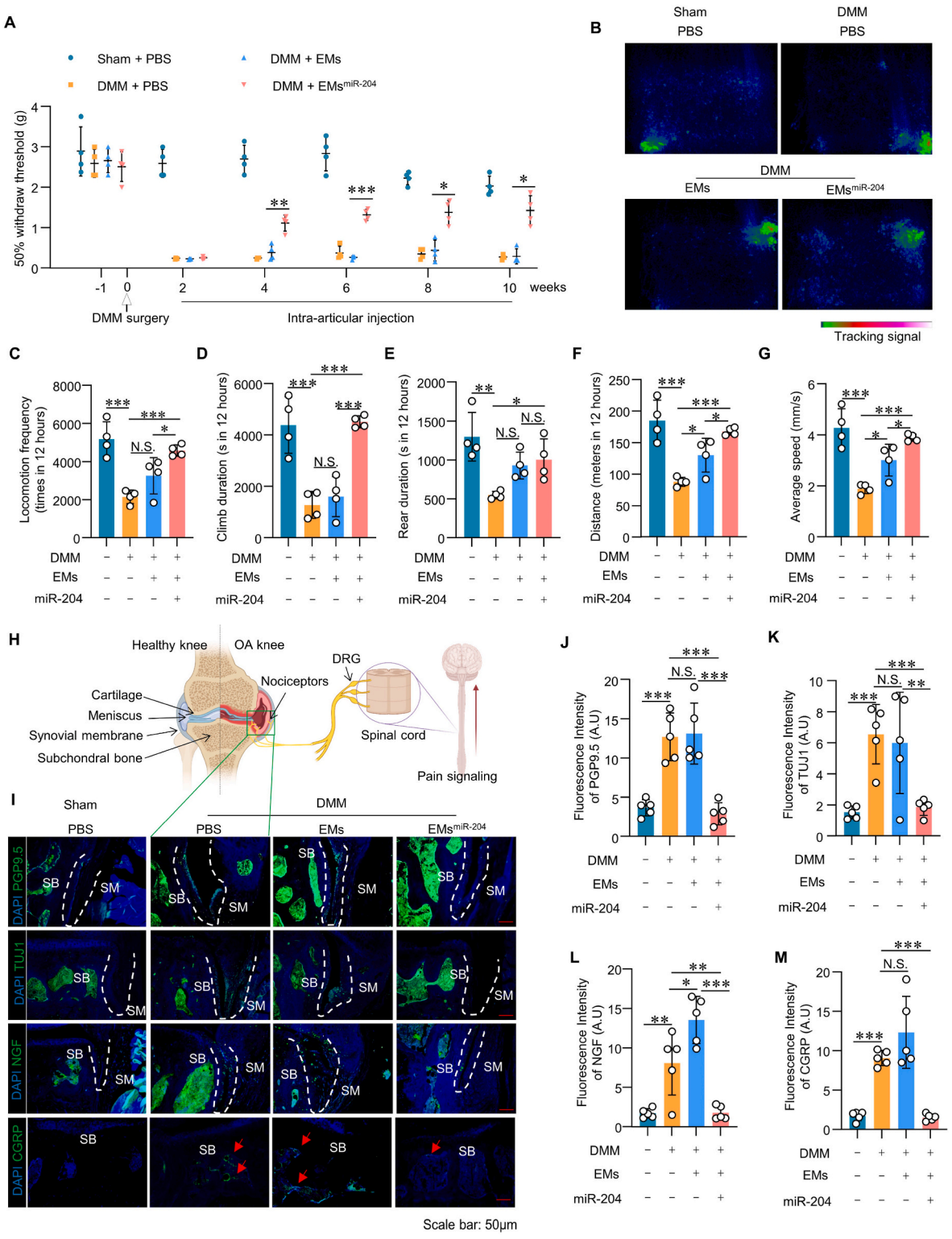


**Fig. 2.** EMs$^{miR-204}$ treatment improves osteoarthritic pain in murine DMM model. (A) The von Frey test showing the sensitivity to mechanical allodynia in Sham or DMM mice with PBS or EMs or EMs$^{miR-204}$ treatment as indicated time points (n = 4). (B–E) The representative images of mice motion track record (B) and analysis of locomotion frequency (C), climb duration (D), rearing duration (E), distance (F) and average speed (G) as indicated groups (n = 4). (H) A schematic diagram illustrating pain signals transmitted from nociceptors in joint to the brain. (I–M) Representative immunofluorescent (IF) images (I) showing PGP9.5, TUJ1, NGF and CGRP expression and quantification of fluorescence intensity of PGP9.5 (J), TUJ1(K) and NGF(L) at the junction area of synovial membrane and cartilage, and CGRP (M) at subchondral bone area in Sham or DMM mice with PBS or EMs or EMs$^{miR-204}$ treatment (n = 5). SB: subchondral bone, SM: synovial membrane *: $P < 0.05$, **: $P < 0.01$, ***: $P < 0.001$, N.S.: no significant difference. Data are represented as mean ± SD. One-way ANOVA followed by Tukey post-hoc test for multiple comparisons (A, C-G and J-M).

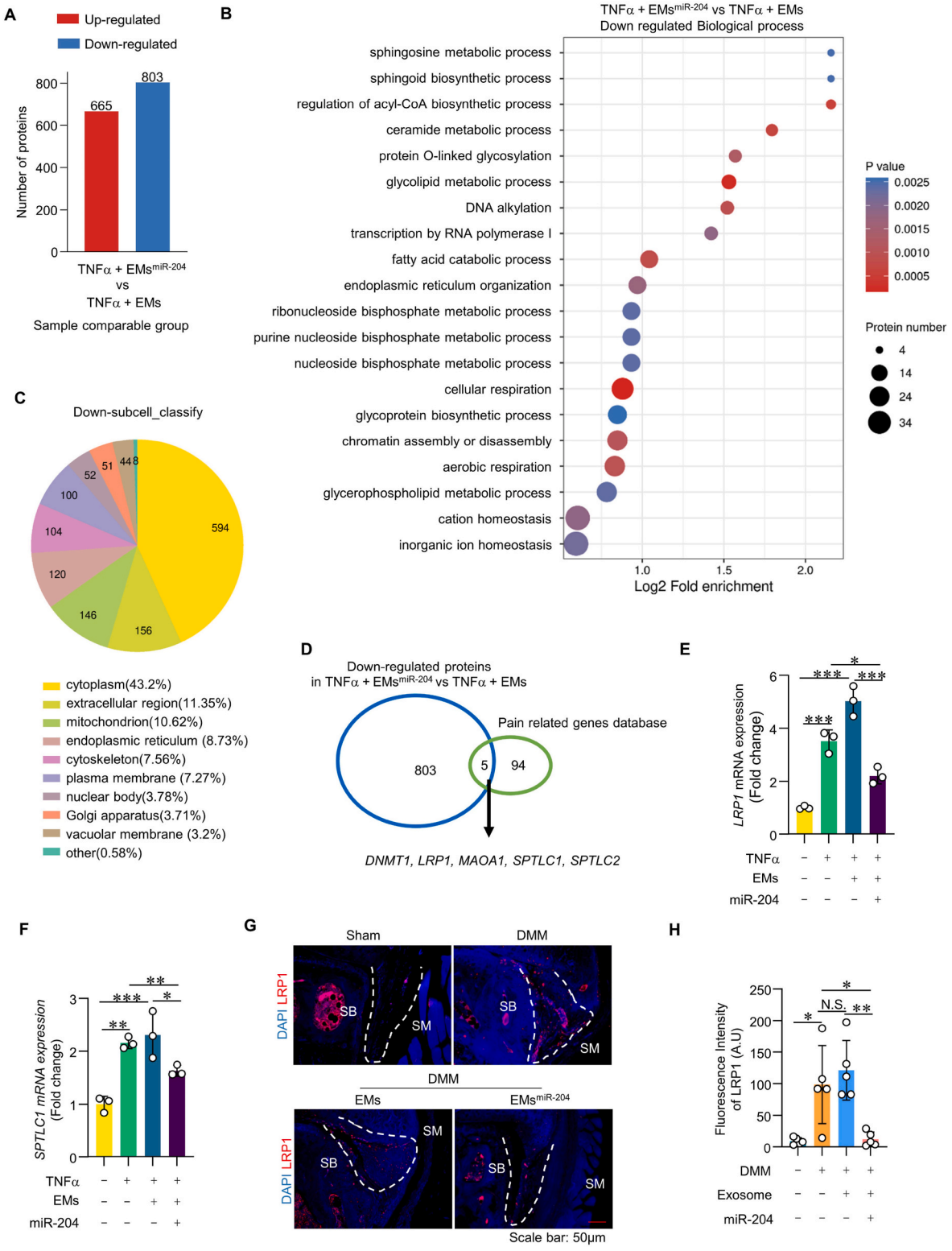


**Fig. 3.** LRP1 involved in pain signaling regulation in chondrocyte with EMs$^{miR-204}$ treatment. (A) The number of proteins in C28/I2 cells with TNF-α+EMs$^{miR-204}$ treatment compared with that in C28/I2 cells with TNF-α+EMs treatment. (B and C) The ratio of down-regulated proteins in TNF-α+ EMs$^{miR-204}$ vs TNF-α+EMs treatment cells using the data of biological process (B) and sub-cell classify (C) analyses. (D) Screening map of down-regulated genes in C28/I2 cells with TNF-α+EMs$^{miR-204}$ treatment and pain related genes database (Table S3). (E and F) qRT-PCR of relative *LRP1* and *SPTLC1* mRNA levels of the groups indicated in C28/I2 cells (n = 3). (G and H) Representative immunofluorescent (IF) staining (G) of LRP1 expression and quantification of LRP1fluorescence intensity (H) at the junction area of synovial membrane and cartilage in Sham or DMM mice with PBS or EMs or EMs$^{miR-204}$ treatment (n = 5). SB: subchondral bone, SM: synovial membrane *: $P < 0.05$, **: $P < 0.01$, ***: $P < 0.001$, N.S.: no significant difference. Data are represented as mean ± SD. One-way ANOVA followed by Tukey post-hoc test for multiple comparisons (E, F and G).

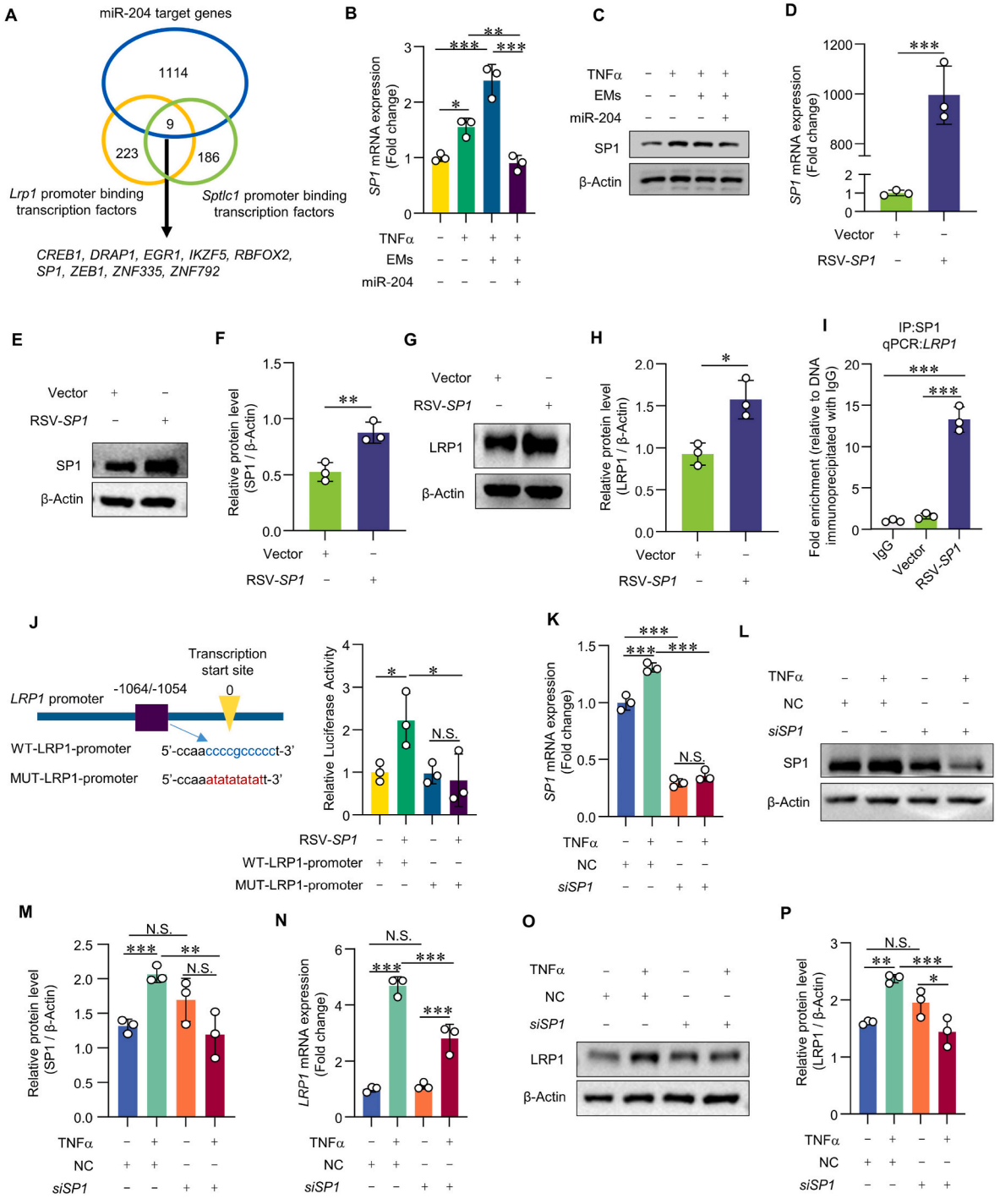


**Fig. 4.** *MiR-204* down-regulate LRP1 expression through inhibition of transcription factor SP1. (A) Screening map of *miR-204* targeting genes and the transcription factors bound to *LRP1* promoter and *SPTLC1* promoter. (B) qRT-PCR of relative *SP1* mRNA levels of the groups indicated in C28/I2 cells (n = 3). (C) Representative immunoblots of SP1 expression of the groups indicated in C28/I2 cells (n = 3). (D) qRT-PCR of relative *SP1* mRNA (A) in C28/I2 cells with RSV-*SP1* transfection (n = 3). (E and F) Representative immunoblots (E) and quantification (F) of SP1 expression in C28/I2 cells with RSV-*SP1* transfection (n = 3). (G and H) Representative immunoblots (G) and quantification (H) of LRP1 expression in C28/I2 cells with RSV-*SP1* transfection (n = 3). (I) ChIP assay was performed using C28/I2 cells transfected with RSV-*SP1* plasmid (n = 3). ChIP-enriched DNA was subjected to qPCR, with the level in IgG group arbitrarily set to 1. (J) LRP1 luciferase activity of the groups indicated, with the level in the blank group arbitrarily set to 1. (K) qRT-PCR of relative *SP1* mRNA (A) in C28/I2 cells with *siSP1* or NC transfection under TNF-α injury (n = 3). (L and M) Representative immunoblots (L) and quantification (M) of LRP1 expression of the groups indicated in C28/I2 cells (n = 3). (N) qRT-PCR of relative *SP1* mRNA (A) in C28/I2 cells with *siSP1* or NC transfection under TNF-α injury (n = 3). (O and P) Representative immunoblots (O) and quantification (P) of LRP1 expression in C28/I2 cells with *siSP1* or NC transfection under TNF-α injury (n = 3). *: $P < 0.05$, **: $P < 0.01$, ***: $P < 0.001$, N.S.: no significant difference. Data are represented as mean ± SD. One-way ANOVA followed by Tukey post-hoc test for multiple comparisons (B, J, K, M, N and P) and two-tailed Student's unpaired *t*-test analysis (D, F, H and I).

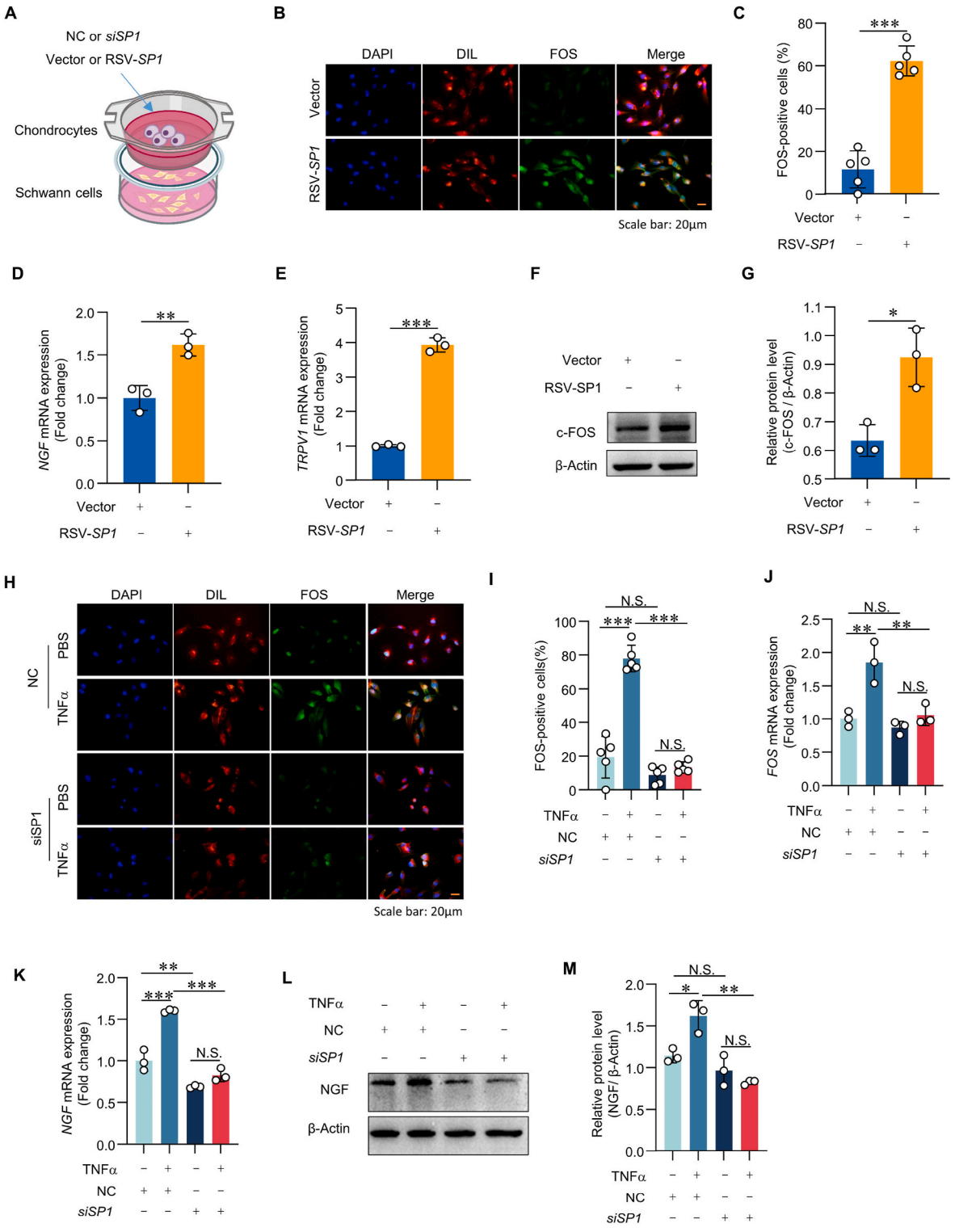


**Fig. 5.** The EMs$^{miR-204}$ inhibit SP1-LRP1 in chondrocyte down-regulating nociceptive neurons activation. (A) A schematic diagram demonstrating C28/I2 cells pretreated as indicated and then co-culture with ipNF95.11 b C cells. (B and C) Representative IF staining (B) of c-FOS expression and quantification of c-FOS fluorescence intensity (C) in ipNF95.11 b C cells (down layer cells) which were co-cultured with C28/I2 cells (up layer cells) pre-transfected with RSV-*SP1* plasmid (n = 5). (D and E) qRT-PCR of relative *NGF* mRNA (D) and *TRPV1* mRNA (E) levels of the groups indicated in ipNF95.11 b C cells (down layer cells) (n = 3). (F and G) Representative immunoblots (F) and quantification (G) of c-FOS expression in C28/I2 cells with RSV-*SP1* transfection (n = 3). (H and I) Representative IF staining (H) of c-FOS expression and quantification of c-FOS fluorescence intensity (I) in ipNF95.11 b C cells (down layer cells) which were co-cultured with C28/I2 cells (up layer cells) pre-transfected with *siSP1* plasmid (n = 5). (J and K) qRT-PCR of relative *FOS* mRNA (J) and *NGF* mRNA (K) levels in ipNF95.11 b C cells (down layer cells) which were co-cultured with C28/I2 cells (up layer cells) pre-transfected with *siSP1* (n = 3). (L and M) Representative immunoblots (L) and quantification (M) of c-FOS expression in C28/I2 cells with *siSP1* transfection (n = 3). *: $P < 0.05$, **: $P < 0.01$, ***: $P < 0.001$, N.S.: no significant difference. Data are represented as mean ± SD. One-way ANOVA followed by Tukey post-hoc test for multiple comparisons (I, J, K and M) and two-tailed Student's unpaired *t*-test analysis (C, D, E and G).

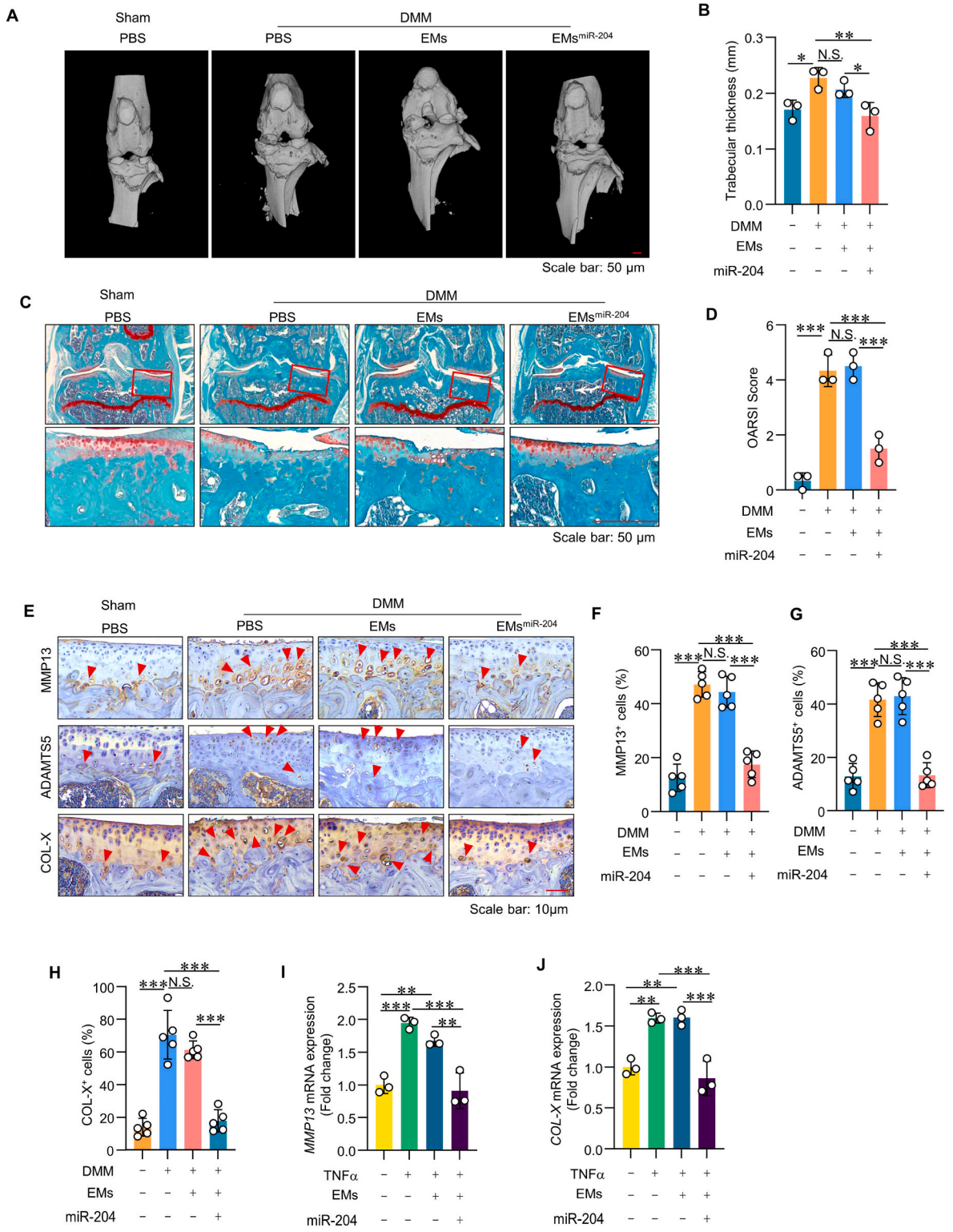


**Fig. 6.** The EMs$^{miR-204}$ alleviates cartilage degradation in DMM-induced OA mice. (A and B) μCT representative images (A) and trabecular thickness quantifications (B) of Sham or DMM mice with PBS or EMs or EMs$^{miR-204}$ treatment (n = 3). (C and D) Representative Safranin O-Fast green staining (scale bar 50 μm) showing histomorphometric changes (C) and OARSI scores (D) in Sham or DMM mice with PBS or EMs or EMs$^{miR-204}$ treatment (n = 3). (E–H) Representative IHC images (E) (scale bar 10 μm) showing expression of MMP13$^+$ (F), ADAMTS5$^+$ (G) and COL-X$^+$ (H) cells in cartilage area of Sham or DMM mice with PBS or EMs or EMs$^{miR-204}$ treatment (n = 3). qRT-PCR of relative *MMP13* mRNA (I) *and COL-X* mRNA (J) levels of the groups indicated in C28/I2 cells (n = 3). *: $P < 0.05$, **: $P < 0.01$, ***: $P < 0.001$, N.S.: no significant difference. Data are represented as mean ± SD. One-way ANOVA followed by Tukey post-hoc test for multiple comparisons (B, D and F-J).

(Scramble siRNA was used as a control, TNF-α was added to the cells) or RSV-*SP1* infection (RSV alone was used as a control) for 12 h, then the cells in upper chamber were co-cultured with the cells in lower chamber (Schwann cell line, ipNF95.11 b C) (Fig. 5A). The FOS has been reported to act as a key marker in pain signaling [17]. Results of IF staining of co-cultured with Schwann cells confirmed that over expression of *SP1* in chondrocytes caused an increase in the accumulation of FOS in Schwann cells (Fig. 5B and C). We also detected high expression of *NGF* and *TRPV1* mRNA levels in Schwann cells co-cultured with RSV-*SP1* infected chondrocytes (Fig. 5D and E). Consistent with above findings, immunoblot results showed high levels of FOS expression in Schwann cells co-cultured with chondrocytes transfected with RSV-*SP1* compared with that in control cells (Fig. 5F and G). We then explored the activation of nociceptive neuron using *SP1* siRNA (*siSP1*) to inhibit *SP1* expression in chondrocytes in the upper chamber. The IF results revealed that FOS positive cells was down-regulated in co-cultured Schwann cells with TNF-α+*siSP1* treated chondrocytes in upper chamber compared with that in TNF-α+NC treated chondrocytes in upper chamber (Fig. 5H and I). qPCR result confirmed *FOS* and *NGF* mRNA was decreased about 50% in Schwann cells co-cultured with chondrocytes which was pretreated with TNF-α+*siSP1* (Fig. 5J and K). Immunoblots also showed that NGF was lower in Schwann cells in lower chamber with *siSP1* transfected chondrocytes (Fig. 5L and M).

### 3.6. The EMs$^{miR-204}$ alleviates cartilage degradation in the OA mouse model

In this study, we demonstrated that EMs$^{miR-204}$ treatment improves osteoarthritic pain in DMM mouse model (Fig. 2), suggesting EMs could serve as an ideal carrier for miR-204 to alleviate cartilage degradation. Compared with DMM mice with PBS or EMs treatment, DMM mice treated with EMs$^{miR-204}$ showed less trabecular thickness (about 25% decrease) by μCT analysis (Fig. 6A and B). While there was no statistical difference of subchondral bone density (BM), bone volume per tissue volume (%, BV/TV), trabecular number (Tb.N.) and trabecular separation (Tb.Sp) between DMM mice treated with EMs alone or DMM mice treated with EMs$^{miR-204}$ (Figs. S10A–D). To further investigate if EMs$^{miR-204}$ protects cartilage degradation in OA, we perform Safranin O/Fast Green staining and found severe defects in the articular cartilage after DMM surgery and increased OARSI scores (a semi-quantitative measure for OA), while treatment with EMs$^{miR-204}$ significantly alleviates cartilage degradation in DMM-induced OA mice and decreased OARSI scores by 66% compared with DMM mice without treatment with EMs$^{miR-204}$ (Fig. 6C and D). IHC results demonstrated significant attenuation on MMP13, ADAMTS5 and COL-X expression in DMM mice treated with EMs$^{miR-204}$ compared with DMM mice without EMs$^{miR-204}$ treatment (Fig. 6E–H). In addition, EMs$^{miR-204}$ treatment also reversed the TNF-α-mediated up-regulation on *MMP13* and *Col-X* expression (Fig. 6I and J).

## 4. Discussion

OA has been recognized as a disease affecting entire joint [17]. Inflammation is often accompanied with peripheral nociceptive nerve proliferation in joint and is the common cause of OA pain [6]. Analysis from a cell biology and evolutionary perspectives, there is no innervation in the space among chondrocytes in healthy knee cartilage, unless OA occurs. As the main cellular component of the joint, the contribution of chondrocytes in OA pain remains unknown. The goal of this study is to determine the role and mechanisms of chondrocytes in mediating neuro-cartilage interaction in OA. It has been reported sensory innervation of lumbar intervertebral discs and sensory nerve ingrowth into the inner layer of intervertebral discs causing low back pain [18]. Peripheral nerve fibers are found sprouting to the synovium in OA mouse model which are correlated with increased joint pain sensation in OA [19]. Consistent with the literature, we found the growth of multiple peripheral nerve fibers into the junction area of the synovium and cartilage by IF staining of neural markers. These findings suggest that this junction area is of great importance in mediating neuro-cartilage interaction and OA pain, and inhibition of nerve ingrowth at this junction area may be a valid approach to suppress OA pain.

Several studies have compared miRNA expression in OA tissue with normal articular tissue. *MiR-34a* KO mice have chondro-protective effect on DMM-induced cartilage damage, suggesting that *miR-34a* promotes joint destruction during OA [20]. Overexpression of *miR-21* in CH8 cells (a chondrocyte cell line) could attenuate the process of chondrogenesis by directly targeting GDF5 [21]. As shown in Fig. 6, in addition to its effect on pain relief, the EMs$^{miR-204}$ also showed significant protective effect on preventing cartilage degradation and osteophyte formation. This is consistent with what we have observed in previous studies, in which we found that intra-articular delivery of *miR*-204 by adeno-associated virus 5 (AAV5) decelerates OA progression in a surgically induced OA mouse model [8]. However, the mechanism of miRNA in OA pain remains elusive. Several studies have utilized NGF-neutralizing antibodies to reduce OA pain and low back pain [22]. Through proteomic analysis and chondrocyte-Schwan cells co-culture experiments, our studies provide new evidence that chondrocytes may be directly involved in the regulation of OA pain through the secretion of cytokines, such as LRP1, which was reported to mediate chemoattraction guide axon and peripheral nerve [23]. LRP1 in Alzheimer's disease has previously been attributed to its regulatory role in both the degradation and production of amyloid β and in regulation of tau uptake and spread [24]. In this study we characterized the role of LRP1 in OA pain and also determined the mechanism of protective effect of miR-204 through down-regulation of SP1 expression and indirectly affecting LRP1 transcription. Consistent with our study, specificity protein 1 (SP1) inhibitor Mithramycin A (MitA) is reported to alleviate OA by inhibiting HIF-2α expression [25].

Alternative option is to inject MSCs expressing miR-204 intra-articularly to determine if similar effect can be achieved for MSCs$^{miR-204}$ compared with EMs$^{miR-204}$. The advantage for using MSCs$^{miR-204}$ is that MSCs alone may already have positive effects on cartilage repair. However, how effective MSCs$^{miR-204}$ can participate in the repairing process of cartilage injury is unknown. We will compare the efficacy of MSCs$^{miR-204}$ with EMs$^{miR-204}$ on OA cartilage repair and osteophyte formation in the future.

In this study, we have tested EMs in delivering *miR-204* for OA treatment. In the future we will test more delivery materials and conduct cross-sectional comparisons to identify a safer and more effective *miR-204* vector for OA treatment. In summary, our findings indicate that EMs could be a potential vector for delivering *miR-204* for OA treatment, and the mechanism of *miR-204* to alleviate OA pain is to inhibit SP1-LRP1 signaling. This study provides us with new drug target for the treatment of OA pain.

## Funding information

This work was supported by the National Key Research and Development Program of China (2021YFB3800800) to L.T. and D.C. This project was also supported by the National Natural Science Foundation of China (NSFC) grants 82030067, 82161160342 and 82250710174 to D.C. and grant 82172397 to L.T. and grant 81874011 to T.W. This project was also supported by the Hong Kong RGC grant HKU-17101821 to W.W.L and D.C.

## Data availability statement

The data that support the findings of this study are available in the main text or the supplementary materials or from the corresponding author upon reasonable request.

## Ethics approval and consent to participate

The animal protocol of this study has been approved by Ethics Committee of the Shenzhen Institute of Advanced Technology, Chinese Academy of Sciences and all experimental methods and procedures were carried out in accordance with the approved protocol to comply with all ethical regulations for animal testing and research (SIAT-IACUC-210618-YYS-CD-A1955). The current study does not involve human subject participation.

## CRediT authorship contribution statement

**Ke Lu:** Data curation, Visualization, Formal analysis, Investigation, Writing – review & editing. **Qingyun Wang:** Data curation, Visualization, Formal analysis, Investigation. **Liuzhi Hao:** Data curation, Visualization, Formal analysis, Investigation. **Guizheng Wei:** Data curation, Visualization, Formal analysis, Investigation. **Tingyu Wang:** Data curation, Formal analysis, Writing – review & editing, Funding acquisition. **William W. Lu:** Data curation, Formal analysis, Writing – review & editing, Funding acquisition. **Guozhi Xiao:** Data curation, Formal analysis, Writing – review & editing. **Liping Tong:** Data curation, Formal analysis, Writing – review & editing, Funding acquisition. **Xiaoli Zhao:** Data curation, Formal analysis, Writing – review & editing. **Di Chen:** Conceptualization, Methodology, Supervision, Writing – review & editing, Funding acquisition.

## Declaration of competing interest

The authors declare that they have no competing interests.

## Appendix A. Supplementary data

Supplementary data to this article can be found online at https://doi.org/10.1016/j.bioactmat.2023.03.010.

## References


[1] G. Zhen, C. Wen, X. Jia, Y. Li, J.L. Crane, S.C. Mears, et al., Inhibition of TGF-beta signaling in mesenchymal stem cells of subchondral bone attenuates osteoarthritis, Nat. Med. 19 (2013) 704–712, https://doi.org/10.1038/nm.3143.

[2] J. Buckland, Osteoarthritis: blocking hedgehog signaling might have therapeutic potential in OA, Nat. Rev. Rheumatol. 6 (2010) 61, https://doi.org/10.1038/nrrheum.2009.270.

[3] Tong L, Yu H, Huang X, Shen J, Xiao G, Chen L, et al. Current understanding of osteoarthritis pathogenesis and relevant new approaches. Bone Res. 10, 60, doi: 10.1038/s41413-022-00226-9 (2022).

[4] M. Zhu, D. Tang, Q. Wu, S. Hao, M. Chen, C. Xie, et al., Activation of beta-catenin signaling in articular chondrocytes leads to osteoarthritis-like phenotype in adult beta-catenin conditional activation mice, J. Bone Miner. Res. 24 (2009) 12–21, https://doi.org/10.1359/jbmr.080901.

[5] R.X. Zhang, K. Ren, R. Dubner, Osteoarthritis pain mechanisms: basic studies in animal models, Osteoarthritis Cartilage 21 (2013) 1308–1315, https://doi.org/10.1016/j.joca.2013.06.013.

[6] P.G. Conaghan, A.D. Cook, J.A. Hamilton, P.P. Tak, Therapeutic options for targeting inflammatory osteoarthritis pain, Nat. Rev. Rheumatol. 15 (2019) 355–363, https://doi.org/10.1038/s41584-019-0221-y.

[7] H.G. Schaible, Nociceptive neurons detect cytokines in arthritis, Arthritis Res. Ther. 16 (2014) 470, https://doi.org/10.1186/s13075-014-0470-8.

[8] J. Huang, L. Zhao, Y. Fan, L. Liao, P.X. Ma, G. Xiao, et al., The microRNAs miR-204 and miR-211 maintain joint homeostasis and protect against osteoarthritis progression, Nat. Commun. 10 (2019) 2876, https://doi.org/10.1038/s41467-019-10753-5.

[9] Z. Ni, S. Zhou, S. Li, L. Kuang, H. Chen, X. Luo, et al., Exosomes: roles and therapeutic potential in osteoarthritis, Bone Res. 8 (2020) 25, https://doi.org/10.1038/s41413-020-0100-9.

[10] S.M. Patil, S.S. Sawant, N.K. Kunda, Exosomes as drug delivery systems: a brief overview and progress update, Eur. J. Pharm. Biopharm. 154 (2020) 259–269, https://doi.org/10.1016/j.ejpb.2020.07.026.

[11] K. Lu, T.S. Shi, S.Y. Shen, Y. Shi, H.L. Gao, J. Wu, et al., Defects in a liver-bone axis contribute to hepatic osteodystrophy disease progression, Cell Metabol. 34 (2022) 441–457 e447, https://doi.org/10.1016/j.cmet.2022.02.006.

[12] J. Li, Y. Wang, D. Chen, R. Liu-Bryan, Oral administration of berberine limits post-traumatic osteoarthritis development and associated pain via AMP-activated protein kinase (AMPK) in mice, Osteoarthritis Cartilage 30 (2022) 160–171, https://doi.org/10.1016/j.joca.2021.10.004.

[13] J. Li, B. Zhang, W.X. Liu, K. Lu, H. Pan, T. Wang, et al., Metformin limits osteoarthritis development and progression through activation of AMPK signalling, Ann. Rheum. Dis. 79 (2020) 635–645, https://doi.org/10.1136/annrheumdis-2019-216713.

[14] J. Shen, J. Li, B. Wang, H. Jin, M. Wang, Y. Zhang, et al., Deletion of the transforming growth factor beta receptor type II gene in articular chondrocytes leads to a progressive osteoarthritis-like phenotype in mice, Arthritis Rheum. 65 (2013) 3107–3119, https://doi.org/10.1002/art.38122.

[15] S.S. Glasson, T.J. Blanchet, E.A. Morris, The surgical destabilization of the medial meniscus (DMM) model of osteoarthritis in the 129/SvEv mouse, Osteoarthritis Cartilage 15 (2007) 1061–1069, https://doi.org/10.1016/j.joca.2007.03.006.

[16] L.A. Vonk, S.F.J. van Dooremalen, N. Liv, J. Klumperman, P.J. Coffer, D.B.F. Saris, et al., Mesenchymal stromal/stem cell-derived extracellular vesicles promote human cartilage regeneration in vitro, Theranostics 8 (2018) 906–920, https://doi.org/10.7150/thno.20746.

[17] P.L. Santos, R.G. Brito, J. Matos, J.S.S. Quintans, L.J. Quintans-Junior, Fos protein as a marker of neuronal activity: a useful tool in the study of the mechanism of action of natural products with analgesic activity, Mol. Neurobiol. 55 (2018) 4560–4579, https://doi.org/10.1007/s12035-017-0658-4.

[18] S. Ohtori, M. Miyagi, G. Inoue, Sensory nerve ingrowth, cytokines, and instability of discogenic low back pain: a review, Spine Surg. Relat. Res. 2 (2018) 11–17, https://doi.org/10.22603/ssrr.2016-0018.

[19] R. Kc, X. Li, J.S. Kroin, Z. Liu, D. Chen, G. Xiao, et al., PKCdelta null mutations in a mouse model of osteoarthritis alter osteoarthritic pain independently of joint pathology by augmenting NGF/TrkA-induced axonal outgrowth, Ann. Rheum. Dis. 75 (2016) 2133–2141, https://doi.org/10.1136/annrheumdis-2015-208444.

[20] H. Endisha, P. Datta, A. Sharma, S. Nakamura, E. Rossomacha, C. Younan, et al., MicroRNA-34a-5p promotes joint destruction during osteoarthritis, Arthritis Rheumatol. 73 (2021) 426–439, https://doi.org/10.1002/art.41552.

[21] Y. Zhang, J. Jia, S. Yang, X. Liu, S. Ye, H. Tian, MicroRNA-21 controls the development of osteoarthritis by targeting GDF-5 in chondrocytes, Exp. Mol. Med. 46 (2014) e79, https://doi.org/10.1038/emm.2013.152.

[22] P. Jayabalan, T.J. Schnitzer, Tanezumab in the treatment of chronic musculoskeletal conditions, Expet Opin. Biol. Ther. 17 (2017) 245–254, https://doi.org/10.1080/14712598.2017.1271873.

[23] L.M. Landowski, M. Pavez, L.S. Brown, R. Gasperini, B.V. Taylor, A.K. West, et al., Low-density lipoprotein receptor-related proteins in a novel mechanism of axon guidance and peripheral nerve regeneration, J. Biol. Chem. 291 (2016) 1092–1102, https://doi.org/10.1074/jbc.M115.668996.

[24] J.N. Rauch, G. Luna, E. Guzman, M. Audouard, C. Challis, Y.E. Sibih, et al., LRP1 is a master regulator of tau uptake and spread, Nature 580 (2020) 381–385, https://doi.org/10.1038/s41586-020-2156-5.

[25] M.C. Choi, W.H. Choi, Mithramycin A alleviates osteoarthritic cartilage destruction by inhibiting HIF-2alpha expression, Int. J. Mol. Sci. 19 (2018), https://doi.org/10.3390/ijms19051411.